JOURNAL OF MATERIALS SCIENCE 37 (2002) 1165–1171

Electrical conductivity and defect structure of CeO_2-ZrO_2 mixed oxide

J.-H. LEE*, S. M. YOON, B.-K. KIM, H.-W. LEE, H. S. SONG
Division of Materials, Korea Institute of Science and Technology, Seoul 136-791, South Korea
E-mail: jongho@kist.re.kr

The electrical conductivity of CeO_2-ZrO_2 system was measured as functions of the temperature and oxygen partial pressure and of the composition. The ionic conduction was prevailing in the ZrO_2 rich phase due to the increase of ionic defect concentration via homovalent doping effect. The enhancement of n-type electronic conductivity was observed in intermediate and CeO_2 rich phase compared with pure CeO_2, which originated either from homovalent doping effect or increase of electronic mobility due to the change of transport mechanism.

1. Introduction

Due to many peculiar electrical and mechanical properties of the ZrO_2 based and CeO_2 based ceramics, a number of studies [1–10] have been conducted. The partially stabilized zirconias are very useful materials for the mechanical and structural application and fully stabilized zirconias are also of interest for many viable electrochemical applications e.g. oxygen sensor, solid oxide fuel cell, steam electrolyser. CeO_2 based electrolytes also have very promising ionic conductivity at moderate temperature (650–800°C) and are known as one of the most prospective material system to replace the zirconia based electrolyte for the low temperature operation of SOFC. Moreover, in now days, ZrO_2-CeO_2 mixed system also spreads of its usefulness to many application fields [11–24]. Especially CeO_2 stabilized zirconia is known to have excellent thermal stability and high toughness compared with other stabilized zirconia system [11, 12]. CeO_2 rich ZrO_2-CeO_2 system also have emerged as a very useful material since they appear to have a higher oxygen storage capacity of the catalysts and thermal stability for the application of exhaust gas treatment for automobile [13–17].

The phase relationships of ZrO_2-CeO_2 system also have been studied by numerous researchers [25–42]. Notwithstanding these a lot of studies, however, it is still not well known and many controversies are found in between literature data. This is known as being due to i) sluggish kinetics at low temperatures below 1400°C and ii) existence of several kinds of metastable phases [32]. The first contributor to the phase relationships of CeO_2-ZrO_2 system was Passerini [25], who has found that a complete solubility existed in between whole compositional ranges of ZrO_2-CeO_2 system and the structure of this solid solution was cubic of the fluorite type. Several years later, Duwez and Odell [26] constructed a tentative phase diagram of CeO_2-ZrO_2 system. They discovered different single or two-phase fields in ZrO_2-CeO_2 system for the first time and completed the phase diagram of ZrO_2-CeO_2 system from XRD analysis. However their proposal was not satisfactory because they did not take into account the tetragonal-cubic transition of zirconia at about 2370°C [27]. The thorough researches in this system were made by Yoshimura *et al*. [28–33]. They proposed that there are two types of tetragonal phase which are formed either from the diffusional phase separation or diffusionless tetragonal-cubic transformation and they presented very viable TTT (Temperature, Time, Transformation) diagram of this system. Most authors agreed to the non-existence of an ordered phase in this system, and only Palguev and Volchenkova [34] and Longo and Minichelli [35] reported the presence of an ordered phase. Duran *et al*. [36] also found the existence of a binary compound $Ce_2Zr_3O_{10}$ at approximately 40 mol% CeO_2. But those studies were not approved until this time. In any case, the phase diagram proposed by Tani *et al*. [30] is now approved as the most acceptable phase diagrams. According to their results, there could be distinguished into three different regions at high temperature (>1200°C); tetragonal ZrO_2 solid solution region, cubic CeO_2 solid solution region, two phase coexistence region.

In this study, the phase relationships in ZrO_2-CeO_2 system were investigated to verify the proposed [30] phase diagram. The electrical properties of ZrO_2-CeO_2 system were also investigated over wide ranges of temperature, oxygen partial pressure and composition to examine the correlation of electrical properties with the defect structures in each composition.

2. Experimental procedure

CeO_2-ZrO_2 ceramics were prepared by the precipitation method. The starting materials were

*Author to whom all correspondence should be addressed.

1M-$ZrCl_2O \cdot 8H_2O$ and 1M-$Ce(NO_3)_3 \cdot 6H_2O$ stock solution. Each hydroxide precursor was precipitated with 6M-NH_4OH solution, The precipitates obtained were washed with water and n-butanol and dehydrated by azeotropic process [43]. Azeotropic process is a very useful method to prevent the particle agglomeration by which controls water being existed between the particles as less as possible. The dried precipitates were calcined at 300°C for 2 h to obtain CeO_2 particles and at 700°C for 2 h to obtain ZrO_2 particles. The dried precipitates were calcined and pressed into a pellet with 24 mm diameter, 1.7 mm thickness and sintered for 2 h in air at 1300°C, which is much lower than normal sintering temperature of 1600°C. Sintered samples were cool down in the furnace fast enough to maintain the phase at sintering temperature. We prepared five different composition of CeO_2-ZrO_2 samples (12 mol%, 50 mol%, 70 mol%, 90 mol%, 100 mol%CeO_2-ZrO_2) and the phases of each samples were determined by X-ray diffraction analysis. (Rigaku, Japan)

The DC four-point probe method was employed to measure the total electrical conductivity. The sintered specimen was cut into the shape of bars using low speed saw (Buehler, USA) and four platinum wire electrodes were wrapped around the sample and nonfluxd platinum paste was painted to improve the contact resistance. S-type (Pt-Pt/Rh 10%) thermocouple was used to measure the temperature of the sample. The current source (Keithley 224, USA) was used to supply the current and the voltage drop across the probes was measured with digital multi-meter (Keithley 197, USA). In order to calculate the electrical conductivity, σ_T, we used following equation

$$\sigma_T = \frac{L}{RA} \tag{1}$$

where L is distance between inner electrodes, A is cross-sectional area of specimen and R is the resistance calculated from the slope of I-V curves, dV/dI. To control the oxygen activity, mixtures of nitrogen and oxygen (N_2/O_2), or carbon dioxide and carbon monoxide (CO_2/CO) were used. We measured the oxygen partial pressure with YSZ oxygen sensor.

3. Results and discussion

3.1. Phase analysis

XRD patterns for sintered specimens at five different compositions are shown in Fig. 1. According to the XRD analysis, ZrO_2-CeO_2 system possesses three different regions; i) tetragonal solid solution region at ZrO_2 rich composition, ii) cubic solid solution region at CeO_2 rich composition, and iii) two phase coexistence regions between region (i) and (ii) at the sintering temperature in air. The phase relations at high temperature are in accordance with the reported phase diagrams [30]. As shown in Fig. 1, cubic solid solution phase was formed at the CeO_2-rich composition (90 m/oCeO_2 composition). In this composition, ZrO_2 is dissolved in CeO_2 and stabilizes the cubic structure. Near the ZrO_2-rich side as for 12 m/oCeO_2-ZrO_2 composition, the tetragonal solid solution phase was formed while both 50 m/oCeO_2 composition and 70 m/oCeO_2

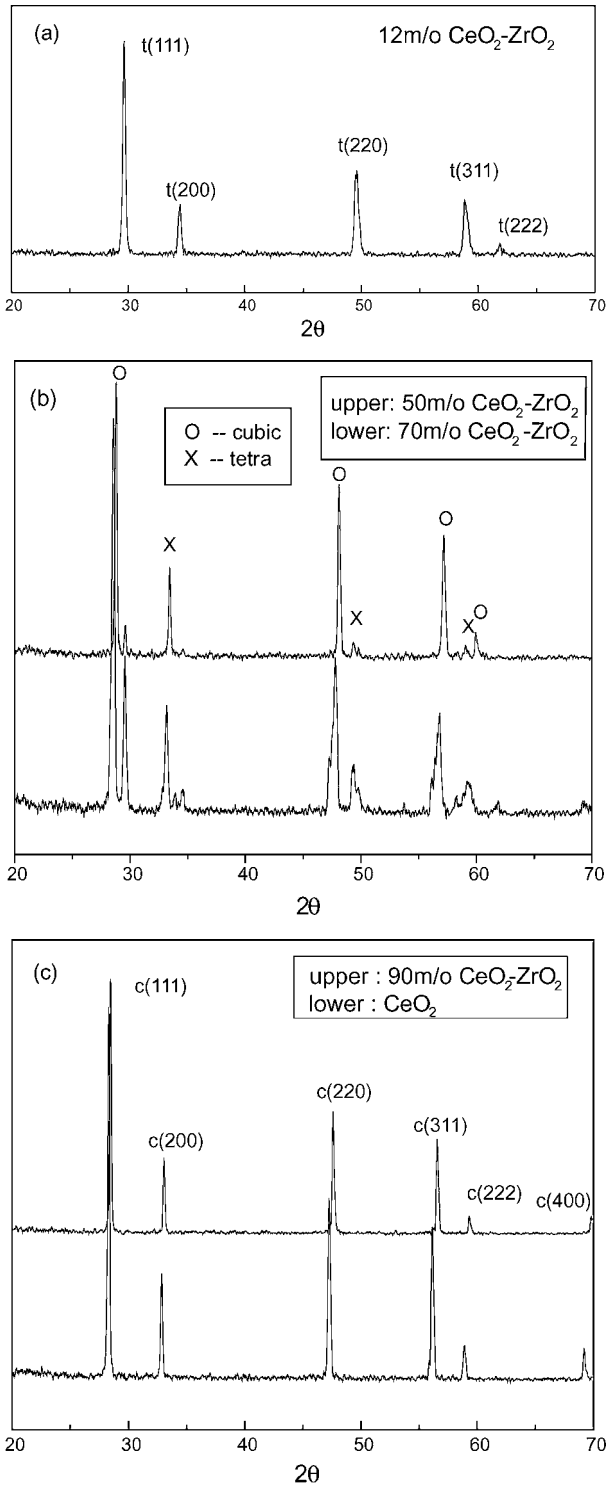

Figure 1 XRD patterns of sintered specimens of CeO_2-ZrO_2; (a) 12 m/oCeO_2-ZrO_2, (b) 50 m/oCeO_2-ZrO_2, 70 m/oCeO_2-ZrO_2, (c) 90 m/oCeO_2-ZrO_2, CeO_2.

composition are correspond to the mixture of these two solid solution phases.

3.2. Electrical property

Fig. 2 illustrates the electrical conductivity of CeO_2-ZrO_2 system as functions of temperature (800–1100°C) and oxygen partial pressure (10^{-16}– 0.21atm). Fig. 2 shows that the ionic conduction is predominant in 12 m/o CeO_2-ZrO_2 system while the n-type electronic conduction is predominant at higher CeO_2 concentration. Fig. 3 shows the electrical conductivity of CeO_2-ZrO_2 system in air atmosphere as a function of CeO_2

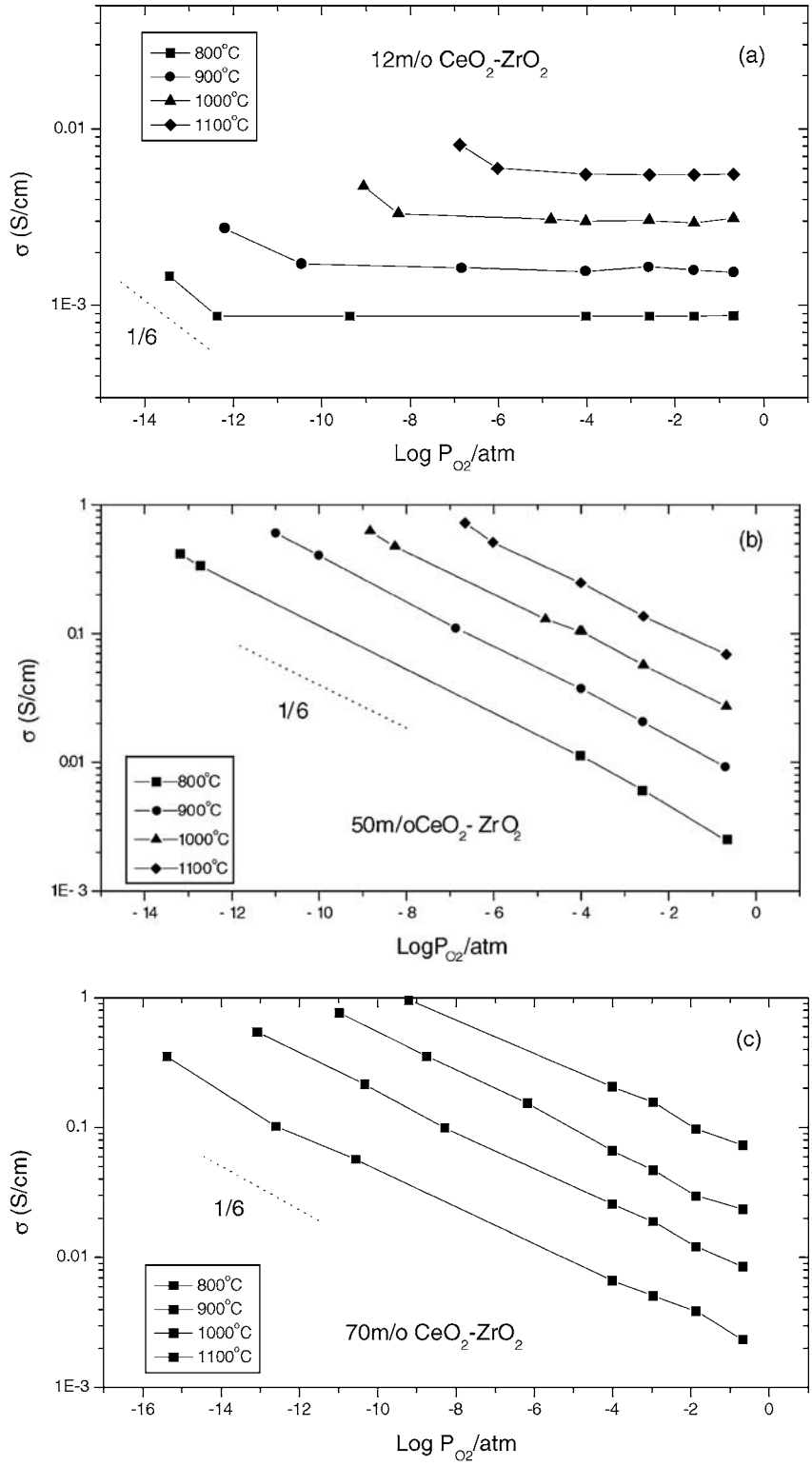

Figure 2 Electrical conductivity as a function of oxygen partial pressure for CeO_2-ZrO_2 system; (a) 12 m/oCeO_2-ZrO_2, (b) 50 m/oCeO_2-ZrO_2, (c) 70 m/oCeO_2-ZrO_2, (d) 90 m/oCeO_2-ZrO_2, (e) CeO_2. (*Continued*.)

concentration. The data of electrical conductivity of pure zirconia in Fig. 3 were quoted from Ref. [44]. Pure zirconia is known to have a p-type electronic conduction behavior in this condition. The electrical conductivity increased as CeO_2 concentration increased and showed the maximum at 90 m/oCeO_2 system and then decreased in pure CeO_2. Fig. 4 shows the activation energy of electrical conductivity in the ZrO_2-CeO_2 system. As shown in Fig. 4, activation energy shows the minimum at 12 m/oCeO_2 and increased up to 40 m/o and then showed nearly composition independent one at higher CeO_2 concentration and pure CeO_2 shows the highest value. These results show good agreement with other literature data [21, 22] as shown in Fig. 4.

3.2.1. ZrO_2-rich CeO_2-ZrO_2 mixed oxide

The enhanced conductivity, comparing with pure zirconia [44], was observed in 12 m/o CeO_2-ZrO_2 system, which shows n-type electronic conduction in low oxygen partial pressure region and typical Po_2 independent ionic conduction in high oxygen partial pressure region.

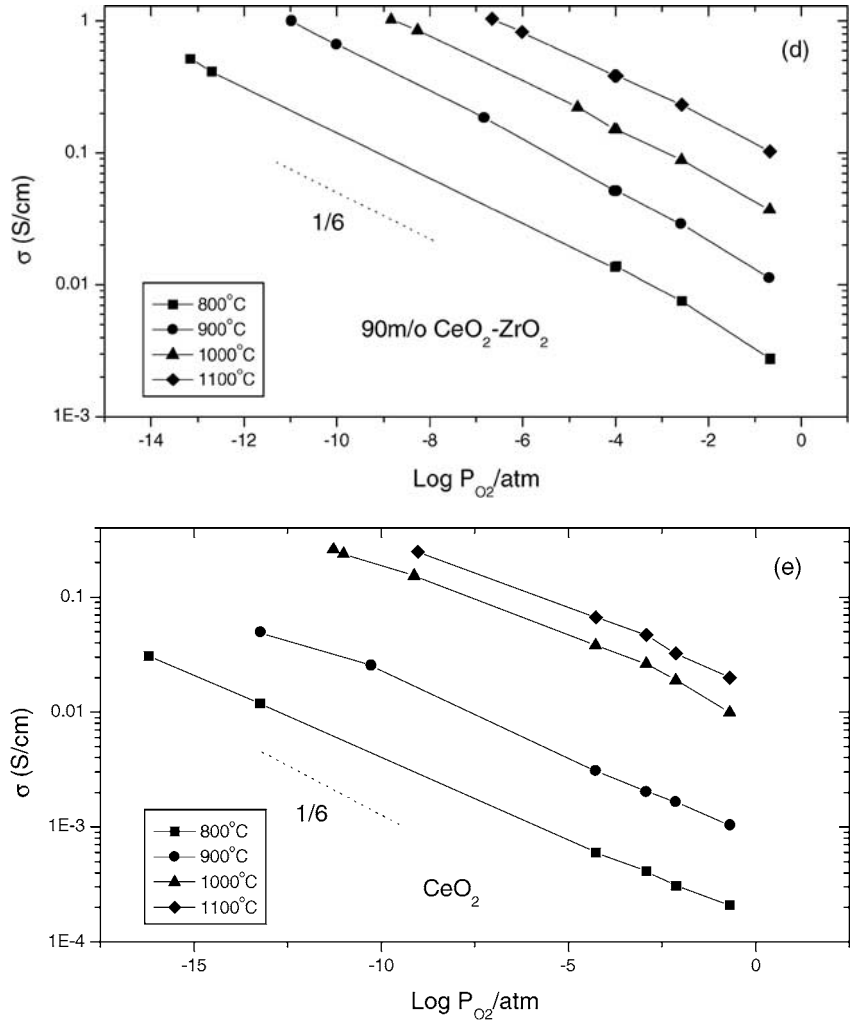

Figure 2 (*Continued*.)

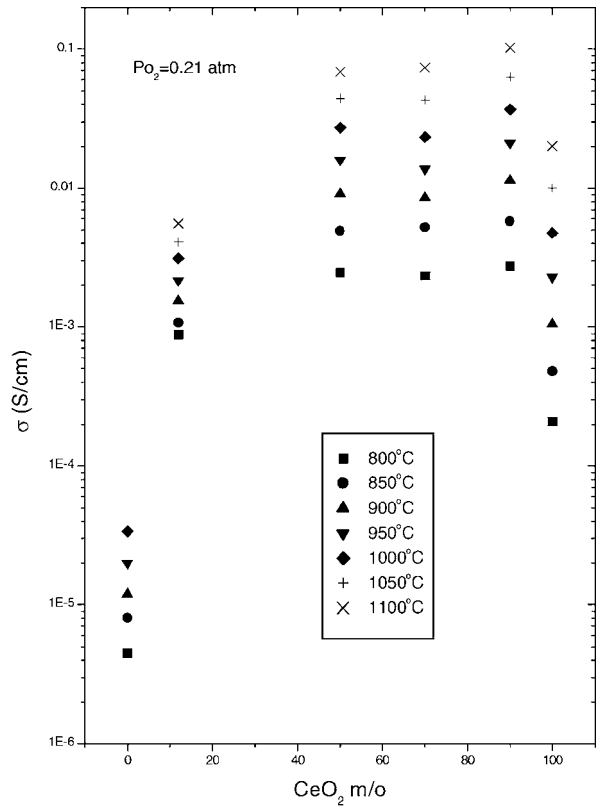

Figure 3 Electrical conductivity as a function of CeO_2 content in air atmosphere at each temperature.

In this system, CeO_2 is dissolved in ZrO_2 and stabilizes the tetragonal form of ZrO_2-CeO_2 solid solution like the other lower valent cation stabilizers (MgO, CaO, Y_2O_3). In general ZrO_2-based materials, lower valent cations (Ca^{2+}, Y^{3+}) have another role to enhance the ionic conductivity by which they substitute normal zirconium sites and create additional ionic charge carriers (in this case, oxygen vacancy) to maintain charge neutrality. The additional creation of the oxygen vacancies over intrinsic anionic Frenkel defects is a very important factor for the application of zirconia as a solid electrolyte.

In the case of CeO_2 stabilized zirconia, however, stabilization process is quite different compared with other general case on addition of aliovalent cation. In this case cerium ion is participating with the same 4+ valence and thus Ce^{4+} ion occupying a zirconium site cannot affect the creation of any additional oxygen vacancies beyond the concentration inherently existed in zirconia.

Nevertheless, it is known that the oxygen vacancy formation can also be encouraged by the strain energy induced by the size difference between dopant and host cations and thus the enhancement of the ionic conductivity can be observed even in the case of homovalent doping [45–47]. In CeO_2-ZrO_2 system, the cerium ion (>1 Å) is larger than the constituent zirconium ion (<0.8 Å) [48] and consequently this size difference

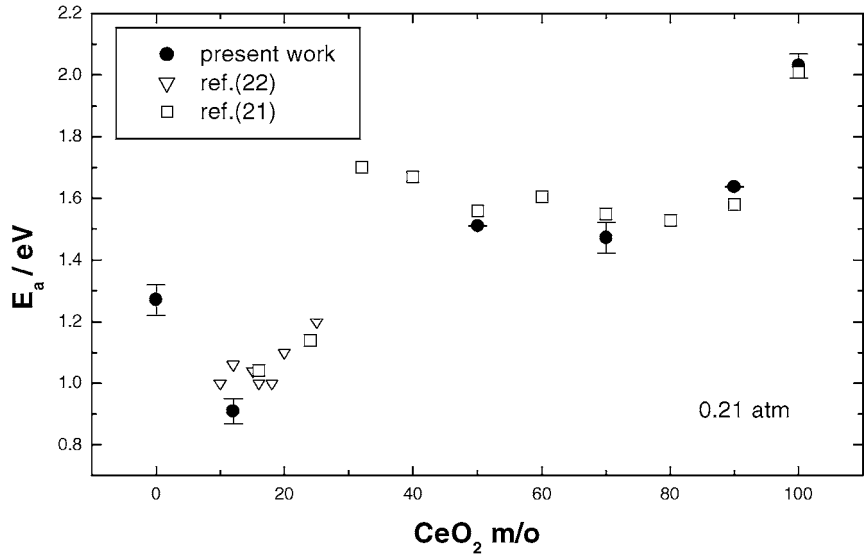

Figure 4 Activation energy as a function of CeO_2 content in air atmosphere.

could encourage the creation of oxygen vacancies. This phenomenon is often called as "size effect". It is normally recognized that the size difference between dopant and host ions causes the distortion of lattice structure and lowers the activation energy of oxygen vacancy formation. Therefore the ionic defect concentration increases and consequently the ionic conduction becomes predominant in 12 m/oCeO_2-ZrO_2 system.

Defect structure of 12 m/o CeO_2-ZrO_2 system has been introduced in our previous paper [49]. It can be summarized as follows. For the defect structure analysis of 12 m/oCeO_2-ZrO_2 system, following two aspects, size effect and reduction of Ce^{4+} to Ce^{3+} are the most peculiar points compared with the other aliovalent doped zirconia. Firstly, as mentioned above, the size effect encourages the creation of oxygen vacancy and enhances the ionic conductivity. As a second, under low oxygen partial pressures, the Ce^{+4} ion is more easily reduced than Zr^{+4} so that n-type electronic conduction surpasses the ionic conduction due to the creation of excess electrons. Except above two points, defect structure analysis is very similar with the case of pure zirconia. The summary of the defect structure of 12 m/o CeO_2-ZrO_2 is given in Table I. The defect structure of the given system can also be applicable for the general ZrO_2 rich ZrO_2-CeO_2 mixed oxides.

As shown in Table I, the region can be distinguished into three with respect to the types of the predominant defects. In the first region denoted by region I, oxygen vacancy and electron which generated from the reduction of cerium ion are predominant defects. In general case, the electrical conductivity is controlled by electronic carrier due to its higher mobility. So it can be expected that the electrical conductivity in this region follows the trend of electron or $[Ce'_{Zr}]$ and consequently shows the n-type electronic conduction and $-1/6$ dependence on log Po_2. This expectation can be confirmed from the experimental results in Fig. 2a, which shows the $-1/6$ dependence of electrical conductivity on log Po_2.

On the other hand, oxygen Frenkel defects are predominant defects in region II. In this region the ionic defects are prevail and ionic conduction is occurred. So the electrical conductivity will show the typical Po_2 independent ionic conduction. This region is specially called as an electrolytic region which can be also observed in zirconia or other doped zirconia system. We could find this electrolytic property from the result in Fig. 2a. The electrolytic property in Fig. 2a is from intrinsic anti-Frenkel defect equilibrium, which is the same as in pure zirconia. But the ionic conductivity of CeO_2-ZrO_2 system is much higher than pure zirconia because the defect formation is encouraged by size effect.

The next high Po_2 region may not be treated here in detail because it was not be verified from the experiment. But one can expect it will show p-type electronic conduction like a pure zirconia.

TABLE I Po_2 dependence of each defect concentration in 12 m/oCeO_2-ZrO_2

Region	I: Low Po_2	II: Intermediate Po_2	III: High Po_2
Charge neutrality	$[Ce_{Zr}'] = 2[V_o^{\cdot\cdot}]$	$[O_i''] = [V_o^{\cdot\cdot}]$	$[h^{\cdot}] = [O_i'']$
$[V_o^{\cdot\cdot}]$	$Po_2^{-1/6}$	Po_2 independent	$Po_2^{-1/6}$
$[O_i'']$	$Po_2^{1/6}$	Po_2 independent	$Po_2^{1/6}$
$[e']$	$Po_2^{-1/6}$	$Po_2^{-1/4}$	$Po_2^{-1/6}$
$[h^{\cdot}]$	$Po_2^{1/6}$	$Po_2^{1/4}$	$Po_2^{1/6}$
$[Ce_{Zr}']$	$Po_2^{-1/6}$	$Po_2^{-1/4}$	$Po_2^{-1/6}$

3.2.2. CeO_2-rich ZrO_2-CeO_2 mixed oxide

Before constructing the defect model in this region, it is better to discuss the defect structure of pure CeO_2that has been treated in many literatures [1–5]. Some reports have proposed the cationic interstitials as predominant defects in CeO_2[1, 2], but in now days from the thorough surveys on the defect structure of CeO_2[3–5], it is normally accepted that the oxygen vacancy is the predominant defect as like previous 12 m/oCeO_2-ZrO_2. We can thus analyze the defect structure of CeO_2 or CeO_2-rich mixed oxide with the similar ways of previous section.

As shown in Fig. 2, both pure CeO_2 and CeO_2-rich CeO_2-ZrO_2 mixed oxide show similar n-type electronic conduction with the same Po_2 dependence which indicate the defect structure of pure CeO_2 and CeO_2-rich CeO_2-ZrO_2 system must be very similar with each other. Moreover, one can expect that the defect structure of CeO_2 rich CeO_2-ZrO_2 system is also similar with previous cases of 12 m/oCeO_2-ZrO_2 system because the situation is not so much different except Zr^{+4} substitute Ce^{4+}. Thus, in this system also, we can expect that three regions, p-type electronic conduction, ionic conduction, n-type electronic conduction region are distinguished as the oxygen partial pressure is changed. Only the difference is we could only observe n-type electronic conduction region from the experiment, which corresponds to the region I in previous section.

According to the results in Fig. 3, the electrical conductivity of 90 m/oCeO_2-ZrO_2 was about ten times higher than pure CeO_2. In previous section, the increase of electrical conductivity of 12 m/oCeO_2-ZrO_2 was explained with the size effect between host and dopant ion. In 90 m/oCeO_2-ZrO_2 system also, the activation energy of the formation of oxygen vacancy would be decreased due to the same reason because the size effect is known to depend on the absolute value of size difference which means either smaller or larger ion can induce the size effect [45–47]. Thus we can expect the increase of ionic conductivity also in 90 m/oCeO_2-ZrO_2 systems as like in 12 m/oCeO_2-ZrO_2 systems. But, in the case of 90 m/oCeO_2-ZrO_2 systems, we can't identify any changes of ionic conductivity or its influence on total conductivity due to the predominant electronic conduction in this condition.

Even though we accept the increase of ionic defect concentration, the increase of n-type electronic conduction in 90 m/oCeO_2-ZrO_2 system can not be explained explicitly. So we have to find another proper explanation about this increment of electronic conduction. In general, the increment of electrical conductivity comes either from the increase of carrier concentration or carrier mobility or both. Recently, Chiodelli *et al.* [21] found that the Seebeck coefficients of pure CeO_2 and 80 m/oCeO_2-ZrO_2 were same at the same experimental condition, which reveals the same electronic carrier concentration between both systems. Thus now we can exclude the increase of electronic carrier concentration in 90 m/oCeO_2-ZrO_2 systems. They also calculated the electron mobility in the 80 m/oCeO_2-ZrO_2 and compared with the one in pure CeO_2. According to their results, the electron mobility in mixed oxide is much higher than in pure oxide that gives a hint to explain the enhancement of electrical conductivity in mixed oxide. At this stage however, we could not verify their explanation explicitly from our study. We only suspect their explanation could be also related with the size effect, that is the electronic mobility can be also influenced by the size effect by which it changed the electronic band structure of CeO_2. But we could not give any concrete conclusion how could the mobility of electron be increased due to the addition of zirconia in detail. Further studies on the influence of size effect on the mobility of charge carrier in homovalent doping case, including partial conductivity measurement will be the subject of next study.

4. Conclusion

According to the XRD phase analysis, 12 m/oCeO_2-ZrO_2 system was corresponded to tetragonal ZrO_2 solid solution phase and 90 m/oCeO_2-ZrO_2 system was corresponded to cubic CeO_2 solid solution phase. On the other hand, 50 m/o, 70 m/oCeO_2-ZrO_2 systems were belonging to two-phase region of above tetragonal and cubic solid solution phases. The electrical conductivity of CeO_2-ZrO_2 system was measured as functions of temperature and oxygen partial pressure with various compositions in order to investigate the conduction type and the defect structure of this system. The electrical conductivity increased as CeO_2 concentration increased and maximum value of electrical conductivity was found at 90 m/oCeO_2 system and then decreased for pure CeO_2. The ionic conduction was prevailing in the ZrO_2 rich phase due to the increase of ionic defect concentration via homovalent doping effect. The enhancement of n-type electronic conductivity was observed in intermediate and CeO_2 rich phase compared with pure CeO_2, which originated either from homovalent doping effect or increase of electronic mobility due to the change of transport mechanism.

References

1. R. N. BLUMENTAL, P. W. LEE and R. J. PANLENER, *J. Electrochem. Soc.* **118** (1971) 123.
2. P. KOFSTAD and A. Z. HED, *J. Amer. Ceram. Soc.* **50** (1967) 681.
3. R. N. BLUMENTAL, F. S. BRUGER and J. E. GARNIER, *J. Electrochem. Soc.* **120** (1970) 1230.
4. O. TOFT SOERENSEN, in "Nonstoichiometric Oxides" (Academic Press, NY, 1981) p. 22.
5. H. L. TULLER and A. S. NOWICK, *J. Phys. Chem. Solids* **38** (1977) 859.
6. P. HAN and W. L. WORREL, *J. Electrochem. Soc.* **142**(12) (1995) 4235.
7. T. KAWADA, N. SAKAI, H. YOKOKAWA and M. DOKIYA, *Solid State Ionics* **53–56** (1992) 418.
8. K. E. SWIDER and W. L. WORREL, *J. Electrochemical Soc.* **143**(11) (1966) 3706.
9. K. KOBAYASHI, Y. KAI, S. YAMAGUCHI, N. FUKATSU, T. KAWASHIMA and Y. IGUCHI, *Solid State Ionics* **93** (1997) 193.
10. A. KOPP, H. NAFE and W. WEPPNER, *ibid.* **53–56** (1992) 853.
11. K. TSUKUMA, *Am. Ceram. Soc. Bull.* **65**(10) (1986) 1386.
12. E. N. S. MUCCILLO and D. M. AVILA, *Ceramics International* **25** (1999) 345.
13. P. FORNASIERO, G. BALDUCCI, R. D. MONTE, J. KASPAR, V. SERGO, G. GUBITOSA, A. FERRERO and M. GRAZIANI, *J. Catalysis* **164** (1996) 173.
14. T. MASUI, T. OZAKI, K. MACHIDA and G. ADACHI, *J. Alloys and Compounds* **303/304** (2000) 49.
15. M. OZAWA, M. KIMURA and A. ISOGAI, *ibid.* **193** (1993) 73.
16. R. D. MONTE, P. FORNASIERO, M. GRAZIANI and J. KASPAR, *ibid.* **275–277** (1998) 877.
17. M. OZAWA, *ibid.* **275–277** (1998) 886.
18. B. CALES and J. F. BAUMARD, *J. Electrochem. Soc.* **131**(10) (1984) 2407.
19. G. A. TOMPSETT, N. M. SAMES and O. YAMAMOTO, *J. Amer. Ceram. Soc.* **80**(12) (1997) 3181.
20. J. JANVIER, M. PIJOLAT, F. VALDIVIESO and M. SOUSTELLE, *Solid State Ionics* **127** (2000) 207.

21. G. CHIODELLI, G. FLOR and M. SCAGLIOTTI, *ibid.* **91** (1996) 109.
22. R. F. REIDY and G. SIMKOVICH, *ibid.* **62** (1993) 85.
23. H. T. HERNANDEZ, J. R. JURADO and P. DURAN, *ibid.* **51** (1992) 147.
24. N. M. SAMMES and Z. CAI, *ibid.* **100** (1997) 39.
25. L. PASSERINI, *Gazz. Chem. Ital.* **60** (1930) 762.
26. P. DUWEZ and F. ODELL, *J. Amer. Ceram. Soc.* **33** (1950) 274.
27. G. M. VOLTEN, *ibid.* **46** (1963) 418.
28. M. YOSHIMURA and H. K. BOWEN, *Am. Ceram. Soc. Bull.* **56** (1977) 301.
29. M. YOSHIMURA, E. TANI and S. SOMIYA, *Solid State Ionics* **314** (1981) 477.
30. E. TANI, M. YOSHIMURA and S. SOMIYA, *J. Amer. Ceram. Soc.* **66** (1983) 506.
31. M. YASHIMA, K. MORIMOTO, N. ISHIZAWA and M. YOSHIMURA, *ibid.* **76** (1993) 2865.
32. M. YASHIMA, H. TAKASHINA, M. KAKIHANA and M. YOSHIMURA, *ibid.* **77**(7) (1994) 1869.
33. M. YASHIMA, M. KAKIHANA and M. YOSHIMURA, *Solid State Ionics* **86–88** (1996) 1131.
34. S. F. PALGUEV and Z. S. VOLCHENKOVA, *Russ. J. Phys. Chem.* **34** (1960) 211.
35. V. LONGO, and D. MINICHELLI, *J. Amer. Ceram. Soc.* **56** (1973) 600.
36. P. DURAN, M. GONZALEZ, C. MOURE, J. R. JURADO and C. PASCUAL, *J. Mater. Sci.*, **25** (1990) 5001.
37. K. TSUKUMA, *Am. Ceram. Soc. Bull.* **65** (1986) 1386.
38. K. TSUKUMA, and M. SHIMIDA, *J. Mater. Sci.* **20** (1985) 1178.
39. J. G. DUH and H. T. DAI, *J. Amer. Ceram. Soc.* **71** (1988) 813.
40. T. SATO and M. SHIMIDA, *Am. Ceram. Soc. Bull.* **64** (1985) 1382.
41. J. G. DUH, H. T. DAI and W. Y. HSU, *J. Mater. Sci.* **23** (1988) 2786.
42. F. F. LANGE, *ibid.* **17** (1982) 255.
43. H-B. KANG and Y-H. KIM, *J. Kor. Ceram. Soc.* **31** (1994) 879.
44. A. KUMAR, D. RAJDEV and D. L. DOUGLASS, *J. Amer. Ceram. Soc.* **55** (1972) 439.
45. K. SHAHI and J. B. WAGNER, JR., *J. Appl. Phys. Lett.* **37** (1980) 757.
46. *Idem.*, *J. Phys. Rev. B* **23** (1981) 6417.
47. *Idem.*, *J. Phys. Chem. Solids.* **43** (1982) 713.
48. G. V. SAMSONOV, in "The Oxide Handbook" (IFI/PLENUM, NY, 1982) p. 2.
49. J.-H. LEE, S. M. YOON, B.-K. KIM, H.-W. LEE and H. S. SONG, *Solid State Ionics* **144** (2001) 175.

Received 21 February
and accepted 2 November 2001